water

MDPI

Article

Fly Ash Waste Conversion to Zeolite and Its Application for Cd^{2+} and Ni^{2+} Adsorption from Aqueous Solutions

Mirela Alina Constantin [1], Lucian Alexandru Constantin [1,*], Florenta Daniela Constantinov [1,2], Valeriu Robert Badescu [1], Cristina Mihaela Nicolescu [3] and Marius Bumbac [3]

[1] National Research and Development Institute for Industrial Ecology ECOIND, 57-73 Drumul Podu Dambovitei Street, 060652 Bucharest, Romania
[2] Chemical Engineering and Biotechnology Doctoral School, National University of Science and Technology Politehnica Bucharest, 1-7 Gheorghe Polizu Street, 011061 Bucharest, Romania
[3] Faculty of Science and Arts, Valahia University of Targoviste, 13 Aleea Sinaia, 130004 Targoviste, Romania
* Correspondence: lucian.constantin@incdecoind.ro

Abstract: Adsorption methods represent a common practice used for heavy metals removal from aqueous solutions. As adsorbent material, zeolites have an excellent adsorption capacity and present low environmental impact. The zeolite used for this study was synthesized from fly ash, a residue generated by thermal power plants, considering the need to reduce fly ash deposits and transform it into useful materials as part of the circular economy. Fly ash conversion to zeolite was performed via a modified hydrothermal method. To investigate the synthetic zeolite structure Scanning Electronic Microscopy, Fourier Transformed Infrared spectroscopy, X-ray diffraction and Raman spectroscopy were used. Chemical composition was revealed by X-ray Fluorescence and thermal behavior was investigated by thermogravimetric analysis. The influence of adsorbent dose and pH upon adsorption capacity of synthesized zeolite for Ni^{2+} and Cd^{2+} was investigated. The effect of contact time on the adsorption capacity of Cd^{2+} and Ni^{2+} was evaluated and it was found that the system reaches equilibrium after 30 min for Ni^{2+} and 60 min for Cd^{2+} due to the saturation of zeolite pores with metallic ions. It was found that the Langmuir model (Lineweaver-Burk equation) better describes the adsorption of both Ni^{2+} and Cd^{2+}. The adsorption kinetics obeys the pseudo-second-order kinetic model (k_2 = 0.0851 g/mg min for Ni^{2+} and k_2 = 0.1780 g/mg min for Cd^{2+}). The adsorption capacity of synthesized was found to be 13 mg/g for Ni^{2+} (initial Ni^{2+} solution concentration = 30 mg/L) and 17 mg/g for Cd^{2+} (initial Cd^{2+} solution concentration = 35 mg/L) at an adsorbent dose of 2 g/L and a contact time of 30 min. Reusability of the zeolite was also tested and it was found that it can be used for 5 cycles. The experimental study revealed that zeolite obtained from fly ash waste generated by a thermal plant represents a viable and sustainable alternative for removal Cd^{2+} and Ni^{2+} from aqueous solution.

Keywords: adsorption; fly ash residue; kinetics; wastewater treatment; zeolite

Academic Editors: Mohammed J.K. Bashir and Devendra Saroj

Received: 8 January 2025
Revised: 1 February 2025
Accepted: 13 February 2025
Published: 18 February 2025

Citation: Constantin, M.A.; Constantin, L.A.; Constantinov, F.D.; Badescu, V.R.; Nicolescu, C.M.; Bumbac, M. Fly Ash Waste Conversion to Zeolite and Its Application for Cd^{2+} and Ni^{2+} Adsorption from Aqueous Solutions. *Water* **2025**, *17*, 593. https://doi.org/10.3390/w17040593

1. Introduction

Water represents the most widely used resource in the majority of the industrial processes that generates wastewater contaminated with different types of pollutants, which can have a negative impact upon environment and human health if it's not treated properly [1]. Considering the increasing demand for pure water the focus nowadays is to find water treatment solutions, if possible, using eco-friendly methods that preserve the natural resources and have an accessible price. Fly ash (FA) is generated by thermal power plants

and represents the residue generated in the incineration process of various solid materials. The composition of FA consists of silica and alumina, which makes it a potential candidate for zeolite synthesis [2,3]. Transforming waste into valuable products is a part of the circular economy concept, also reducing the amount of waste that ends up in landfill [4].

Zeolites are a type of aluminosilicates having a tetrahedron crystalline structure composed of ions such as silicon, aluminum, and oxygen bonds (representing the negative charge) and other metallic ions such as sodium, potassium, calcium (representing the positive charge); these cations can be replaced with other ions by ionic exchange [5,6]. The general formula of natural zeolites is (M_x^+, M_y^{2+}) $[Al_{(x+2y)}$ $Si_{n}{}_{(x+2y)}$ $O_{2n}] \times mH_2O$ [7]. The basic unit tetrahedron can be rearranged in different crystalline structures depending on the number of rings (4,6,8) and those formations have channels or cavities that allow the passage of molecules with sizes between 2.8 and 7.7 Å [8]. This porous structure allows them to be used as adsorption materials for heavy metals removal, while their ionic charge can be beneficial in ion-exchange processes [6,9,10].

Zeolites presents cation exchange capacity (CEC) depending on their framework structure, charge density of anionic framework, ion size and shape, ionic charge and solution concentration. Moreover, zeolites are considered eco-friendly catalysts for various applications.

Some studies suggested that combining a sodium zeolite with an organic surfactant (hexadecyltrimethylammonium—HDTMA), making it suitable for removing organic pollutants from aqueous solutions in the range between 55–75,000 mg/L in addition to metallic ions removal [11]. Due to their CEC zeolites can act as good cation exchanger, but their limited pore size when in contact with a HDTMA solution the surface active sites are occupied by these large cations. Such surfactant-modified zeolites (SMZ) are efficient sorbents for many types of pollutants, including anionic and organic compounds.

Zeolites have been used in a variety of applications, including the removal of volatile organic compounds and hydrocarbons [12], the adsorption of inorganic [13] and organic pollutants by others [14], Zeolites are also important for waste water treatment technology because it has very good properties with important lattice stability [15], and the removal of phosphate ions [16]. Another interesting application is the use of zeolites as fertilizers and the study of the effect of zeolites on soil composition [17].

Beside zeolites, metal-organic frameworks (MOF) represent other absorbents used for metals removal from aqueous media, due to their excellent absorption efficiency for removal of heavy metals from polluted water. MOF presents the advantages of larger surface area, high porous structure and better functionality. MOF were used for removal of toxic metals such as arsenic, chromium and lead [18].

Graphene-based aerogels (GBAs) have also emerged in the last years as excellent materials for removal of metals from aqueous media. Moreover, GBAs proved to be suitable for removal of other type of contaminants along with metal ions, often in a synergetic way [19].

Reaction time and temperature influence the conditions for obtaining zeolites. Types such as Na-A, Na-Y, Na-X, sodalised zeolites, cancrinites, chabazites and analcimes can be obtained by different methods [20]. NaP1_FA zeolite type and zeolite-carbon composite (NaP1_C) can be used as an adsorbent for erythromycin removal from aqueous solutions [21].

The adsorption capacity depends on the pore size structure. In general, zeolites presents a good adsorption capacity, due to a large specific surface area, large pore volume and good thermal stability. In the synthesis of zeolites an important role is played by both the initial conditions and the material from which it comes, due to the fact that the fly ashes that are used as a source has a different composition in respect to Al_2O_3 and SiO_2. Other important parameters are stirring, the time of ageing, heating time, crystallization

temperature, calcination temperature, charge of entering ions, charge density, and initial concentration of contaminants in solution, initial pH and temperature of solution [22].

Researchers developed various methods for synthesis of zeolites [23–26] and demonstrated the capacity of zeolites to remove heavy metals from aqueous media [27,28].

The quality of the obtained zeolites and especially the quality of the crystalline phases is influenced by the main working conditions like: temperature, process time, pH and composition of the fly ash (ratio between SiO_2 and Al_2O_3) [23]. Zeolitization processes depends on several parameters as the content of NaOH (ratio fly ash/NaOH) with the specification that a large quantity of NaOH doesn't help the process of growing and implicitly zeolitization [29].

Usually in wastewater are found metals who can pollute the environment. Nickel, cadmium, chromium, lead, zinc and copper are the most important and their removal becomes a priority during last decades. Various methods have been reported in the literature on metals removal such as: filtration, ultrafiltration, reverse osmosis, electro dialysis, electrocoagulation, adsorption, ion exchange.

Among other applications the most common is adsorption for wastewater treatment. It is well known that synthetic zeolites are preferred because they present a good selectivity and are reusable.

Synthetic zeolites are obtained in various ways according to the Circular Economy Concept [30]. The main methods are hydrothermal fusion, convection hydrothermal and hydrothermal method using microwave waves [23]. The main goal of this work was to synthesize zeolite starting from fly ash via hydrothermal method, its characterization and investigation of its adsorption capacity, adsorption isotherms and pseudo-first-order and pseudo second order kinetic models. This work focused on studying the adsorption capacity of heavy metals using zeolite synthesized from fly ash.

This study present an alternative to convert waste (fly ash in this case) to useful material (zeolite) with a good selectivity and reusability. This process has a good environmental effect and a spread utilization in different treatment technologies.

2. Materials and Methods

2.1. Zeolite Preparation Method

In order to generate a homogeneous material, the FA was grounded manually and treated preliminary by ultrasonic equipment (ISOLAB Laborgerate GmbH, Eschau, Germany) for 1 h at 50 °C to remove any unburned residues. The material was dried at 90 °C for 24 h and treated with hydrochloric acid (HCl) 20% (Sigma Aldrich Chemie GmbH, Steinheim, Germany) to remove impurities such as Fe_2O_3. For 2 h was stirred constantly at 80 °C. At the end of the acid treatment, the solid was filtered and washed with deionized water (Milli-Q Integral 15, Merck, Millipore, Darmstadt, Germany) to ensure that the residual acid has been removed and dried overnight at 105 °C. To enhance the zeolitization, for this work we used fusion method with hydrothermal method [31] in order to improve the quality of zeolite synthesis.

The solid mass (previously obtained) was mixed with sodium hydroxide (sodium hidroxyde:fly ash = 2.25 mass ratio) (Chem-Lab, Zedelgem, Belgium), burned for 1 h at 550 °C in a muffle furnace (Heatherm OHM 100-S, Thermo Fischer, Waltham, MA, USA) and treated with deionized water for 12 h (at 300 rpm) after cooling down. The mixture has been crystallized at 80 °C for 4 h followed by washing step (with deionized water until pH = 10) and dried over night at 105 °C.

2.2. Zeolite Characterization

The raw material (waste fly ash) used in this experimental study was purchased from a Romanian thermal power plant. Preliminary results on chemical composition, thermal behavior, morphology of fly ash were reported in a previous study [32] and it was observed its potential to generate a zeolite with a good adsorption capacity.

The chemical composition of the zeolite was determined by X-ray fluorescence (XRF) using Rigaku NEX CG EDXRF spectrometer (Applied Rigaku Technologies Inc., Cedar Park, TX, USA). The surface morphology of the zeolite was visualized using a scanning electron microscope (SEM), recorded with a Quanta FEG 250 (Thermo Fischer, Waltham, MA, USA). The Quanta FEG Scanning Electron Microscope produces enlarged images of a variety of specimens, achieving magnifications of over 100,000× providing high resolution imaging in a digital format. Thermogravimetric analysis is using A Netzsch STA PC 409 equipment. Working atmosphere was synthetic air, 100 mL/min in alumina crucibles. The heating program was 35−1200 °C with a heating speed of 10 °C/min.

Zeolite was analyzed also using Thermo's Fourier Infrared Spectrometer (FT-IR) Vertex 80 infrared spectrometer (Bruker, Ettlingen, Germany) and a micro-RAMAN equipment—XploRA PLUS acquired from HORIBA (Kyoto, Japan).

The X-ray Diffraction (XRD) was used to confirm the crystalline structure of the synthesized material from fly ash. For data acquisition, a monochromatic Cu Kα radiation (λ = 1.54056 Å) was used, generated by a fixed anode X-ray tube operated at 40 kV and 30 mA of the Ultima IV (Rigaku, Japan) diffractometer. Recorded X-ray patterns of the powder samples were obtained in the 2-theta range of 10–100 degrees, using Bragg-Brentano geometry with continuous scan mode at 1 degree/minute speed and 0.02-degree step width. Then, the PDXL version 2.2. software and the ICDD data base $PDF_4{}^+$ version 2023 were used for XRD data analysis.

The concentration of $Ni^{2+}$and Cd^{2+} was determined by an Atomic Absorption Spectrometer (AAS)—PinAAcle 900 T (Perkin Elmer, Shelton, CT, USA).

2.3. Adsorption Experiments

2.3.1. Langmuir Isotherms

In 1918 Langmuir describes the balance between adsorption and desorption process and proposed an equation, first scientifically derived isotherm [33]. This equation starts from the premise that the surface of the adsorbent is homogeneous, meaning the adsorption energy is uniform throughout surface and not dependable on the surface overlay. Langmuir is satisfied for homogenous surface that ignores adsorbate—adsorbate interaction. In addition, the molecules are adsorbed on specific sites and each site is able to adsorb just one specie. For the present work, Langmuir equation models expressed as Linewear-Burk and Haes Woolf forms were used (Table 1).

Table 1. Linear forms of the Langmuir isotherm.

Linear Model	Linear Form Equation
Linewear-Burk	$\frac{1}{q_e} = \frac{1}{q_m} + \frac{1}{q_m K_L}\frac{1}{C_e}$
Hanes-Woolf	$\frac{C_e}{q_e} = \frac{1}{q_m K_L} + \frac{1}{q_m}C$

Note(s): Where: q_e—adsorption capacity at equilibrium—number of metallic ionic adsorbed per unit of solid mass (mg/g); q_m—maximum adsorption capacity of solid (mg/g); C_e—the equilibrium concentration of metallic ions in solution (mg/L); K_L—equilibrium parameter Langmuir (L/g).

The reciprocally of the variables q_e and C_e for regression is taken into account within linear isotherms of Langmuir form 1 and 2. This leads to regression problems dominated

by low values of q_e and C_e. This observation can be applied or the other linear forms of the Langmuir isotherms.

For the Langmuir forms, use the variable q_e for the definition of both independent and dependent variables, which may lead to inconsistent definitions of measurement fluctuations or use variable C_e for the definition of both independent and dependent variables.

This feature of the model formulation can lead to a good correlation between the independent and dependent variables with a high correlation of the model predictions with the experimental data. The plot of C_e/q_e versus C_e usually leads to very good model fits the experimental data and is usually selected as the best linear form of the Langmuir isotherm.

2.3.2. Freundlich Isotherms

The adsorption equilibrium was proposed by Freundlich in 1906 and is known as Freundlich isotherm. It is considered as an empirical equation and can portray adsorption for heterogeneous surfaces. It is different from the Langmuir isotherm because does not lead to Henry's law for dilute concentrations. A heterogeneous adsorption system is better described by Freundlich isotherm which applies to multilayer adsorption, with non-uniform adsorption heat distribution and non-uniform affinities over the heterogeneous surface.

Also does not predict the existence of a maximum adsorbed value, as the concentration in the fluid phase increases. The Freundlich isotherm is defined in Equation (1) and the linear form, obtained through a logarithmic transformation, is presented in Equation (2).

$$q_e = K_F \text{ x } C_e^{(1/n)} \quad (1)$$

$$\text{Ln}(q_e) = \text{Ln}(K_F) + (1/n) \times C_e \quad (2)$$

where:

C_e—the equilibrium concentration of metallic ions in solution (mg/L);

K_F—Freundlich adsorption constant (mg/g);

1/n—empirical constant (mg/L) positive and smaller than 1.

2.3.3. Kinetic Modelling

To study process kinetics pseudo-first-order (Lagergreen equation) and pseudo-second-order kinetics models were used.

The pseudo first order kinetic model is represented by the following equation

$$\text{Log}(q_e - q_t) = \text{Log}q_e - k_1/2.303 \text{ t} \quad (3)$$

The pseudo-second order kinetic model is represented as:

$$dq_t/dt = k_2(q_e - q_t)^2 \quad (4)$$

$$t/q_t = 1/(k_2 \times q_e^2) + (1/q_e) \times t \quad (5)$$

where:

k_1 = pseudo first order rate constant (min^{-1});

t = time (min);

k_2—pseudo-second-order rate constant (g/mg/min);

q_e—the amount of solute sorbed per mass of sorbent (mg/g);

q_t—is the capacity of metal adsorption at any time (mg/g).

3. Results and Discussion

3.1. Zeolite Synthesis

Preliminary treatment of FA. Waste FA was subject to ultrasound treatment for 1 h at 50 °C in order to eliminate any unburned residue. Resulted material was dried at 90 °C for 24 h and then was subject to five cycles of HCl solution treatment—drying at 70 °C for 1 h in order to remove impurities. In the end fly ash was washed with deionized water in order to remove residual acid, dried at 105 °C and further calcinated at 550 °C for 1 h in order to remove carbonated residues.

Hydrothermal treatment. Preliminary treated fly ash and NaOH powder were thermally treated at 550 °C, the mineral structure of fly ash was destroyed and a large number of silicon and aluminum sources were released. In the meantime, the polymerization reaction generates a silica aluminate gel. The gel was depolymerized and structural rearranged under the action of ions. Zeolite is formed into a crystalline structural unit and in the end these units are polymerized and joined to form zeolite crystals.

The experimental diagram of zeolite preparation is presented in Figure 1.

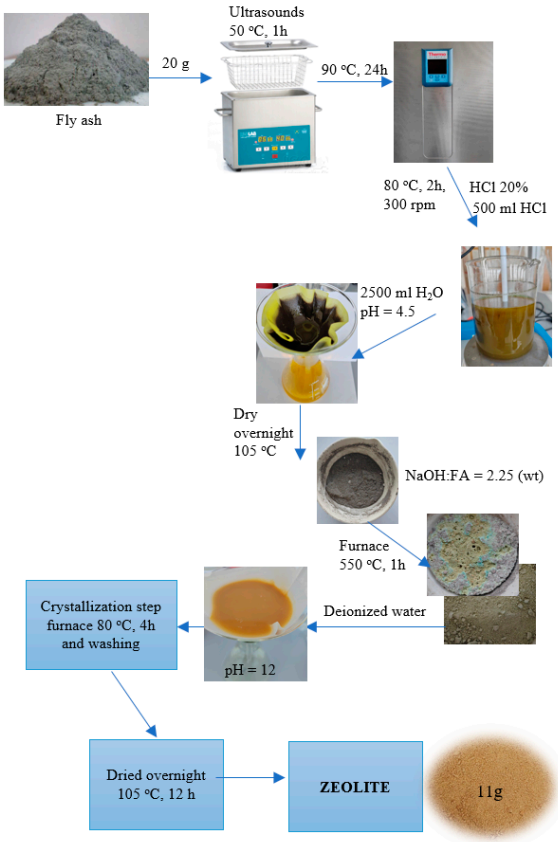

Figure 1. The experimental diagram of zeolite preparation from fly ash.

3.2. Zeolite Characterisation

3.2.1. X-Ray Fluorescence Analysis

The chemical composition of the coal fly ash was determined using X-ray fluorescence (XRF) (Table 2). The major compounds in zeolite sample include major elements Al_2O_3, SiO_2, Fe_2O_3, Na_2O. Minor compounds include TiO_2, MgO, K_2O, SO_3, CaO, ZnO, MnO, CuO, BaO, Cl, NiO and Cr_2O_3.

Table 2. Result of X-ray fluorescence analysis (XRF) of zeolite synthetized.

XRF Element	(wt.%, Dry Basis)
TiO_2	0.71
Al_2O_3	20.60
SiO_2	34.22
MgO	1.30
K_2O	0.37
SO_3	0.47
CaO	0.71
Fe_2O_3	5.15
Cl	0.03
BaO	0.03
ZnO	0.01
Na_2O	21.84
MnO	0.03
CuO	0.01
NiO	0.01
Cr_2O_3	0.01
LOI	13.87

Table 2 lists the chemical composition of zeolite showing that it contains more SiO_2 (34.22%), Al_2O_3 (20.60%) and Na_2O (21.84%). SiO_2/Al_2O_3 ratio calculated from XRF results was found to have a value of 1.66, which is suitable for synthesis of an aluminum rich zeolite. Na:Al:Si calculated molar ratio is 1:0.573:0.810.

3.2.2. Scanning Electron Microscope Analysis

The morphology of the zeolite particles found to be with irregular shape and is shown in Figure 2. This demonstrate that after melting particle of flying ash with NaOH followed by hydrothermal treatment, spheres become cubic crystal structures. NaOH destroys the original crystal structure of fly ash and dissolves a large amount of silicon and aluminum. Nucleation process occurs rapidly on the surface of particles and forms unique crystal structure [34]. Zeolite is a sodium aluminum silicate hydrate.

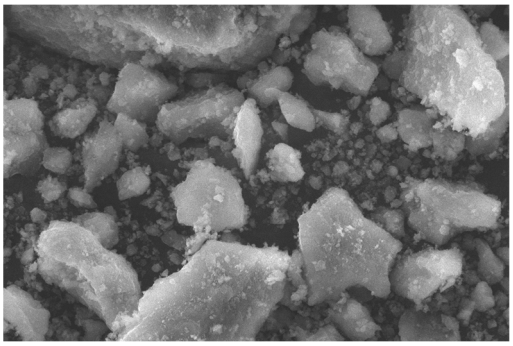

Figure 2. SEM images of synthetized zeolite from fly ash.

3.2.3. Thermogravimetric Analysis

Thermogravimetric analysis (TGA) shows the derivative TG curve of the synthetic zeolite (Figure 3).

In the temperature range of 70–335 °C, the synthetic zeolite exhibits fast loss rate corresponding weight loss, attributed to the overflow of adsorbed water and water elimination from the synthetic zeolite sample. The synthetic zeolite shows a relative lower degradation rate between 335 °C and 730 °C and after 730 °C, the weight is almost the same. The results

showed a difference of mass loss percentages of 13.62% between 105 °C and 950 °C, which correlates with the loss of ignition of 13.87%.

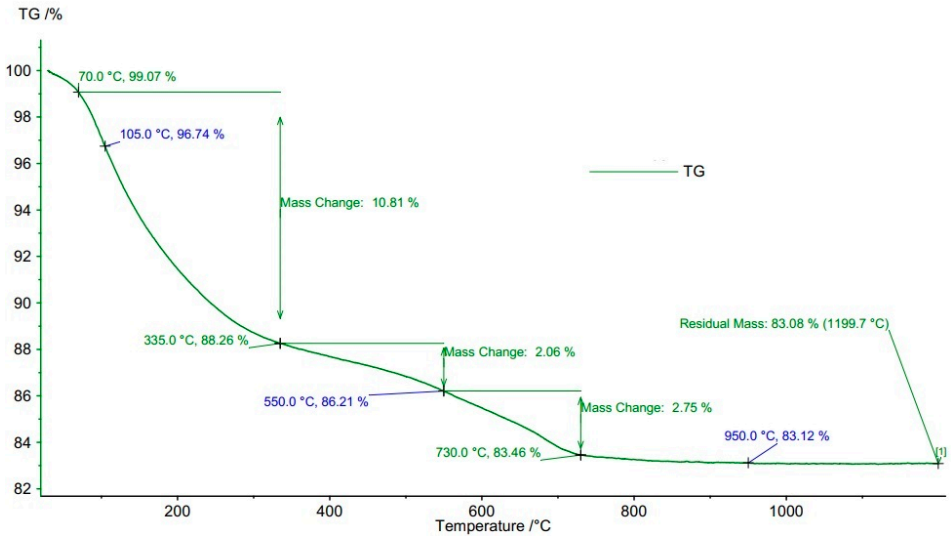

Figure 3. TGA of zeolite from fly ash at 10 °C/min.

3.2.4. Fourier Transformed Infrared Spectroscopy (FTIR) Analysis

FT-IR spectra of fly ash and zeolite is shown in Figure 4 and is consistent with forming a zeolite from the ash containing silica and alumina. The presence of O-H stretching (large band at 3200–3500 cm^{-1}) and O-H bending vibrations (1630 cm^{-1}) indicate hydroxyl groups (OH) formed in the material structure [34]. The zeolite structure formation is also confirmed by the small bands in the 600–700 cm^{-1} domain. This region is generally assigned to metal-O bending vibrations (possibly Si-O or Al-O). Zeolites have a framework structure composed of SiO_4 and AlO_4 tetrahedra linked together by oxygen atoms. Given the presence of O-H bands and bands in the 600–700 cm^{-1} region, it's likely that your thermally treated ash successfully converted into a zeolite structure.

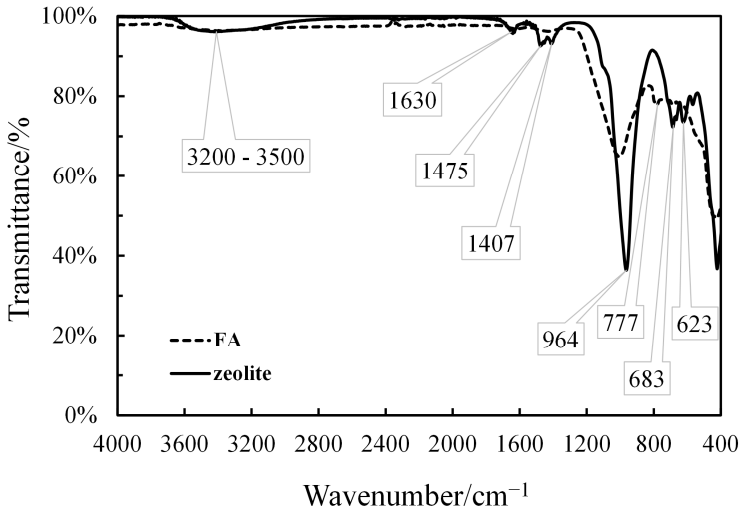

Figure 4. Infrared absorption spectra of fly ash and synthetic zeolite.

The characteristic peak 400 cm^{-1} are attributed to the tensile vibrations of Al-O-Al.

The treatment with hydrochloric acid followed by thermal treatment could definitely contribute to the observed changes in the IR spectrum and potentially lead to a more ordered zeolite structure. HCl can dissolve metal oxides and other mineral phases in the

flying ash besides silica and alumina expand more. This can lead to a cleaner starting material for zeolite synthesis, potentially allowing for a more ordered framework to form during thermal treatment.

HCl can also partially leach out aluminum from the ash. While this might seem counterintuitive for zeolite synthesis (which requires aluminum), controlled dealumination can actually be beneficial. It can help to create defects in the initial framework, which can then be rearranged during thermal treatment to form a more ordered structure with improved porosity and accessibility.

3.2.5. Raman Analysis

Raman analysis investigated the chemical structure of the fly ash, providing information about the dissolution and transformation process from polymers (aluminosilicate) to monomers and then by structural rearrangement to zeolite. The Raman Spectrometer (HORIBA, Kyoto, Japan) was equipped with Integrated Imaging spectrometer with 4 gratings mounted on motorized turret for full resolution, range and coverage (gratings: 600 g, 1200 g, 1800 g) and Olympus Microscope BX43 with 5× (NA = 0.1; WD = 19.6 mm), 10× (NA = 0.25, WD = 10.6 mm) and 100× (NA = 0.9, WD = 0.21) objectives. LabSpec6 software controls a motorized 2-position "visualization/measurement" switch for automatic positioning. The acquisition time was set at 30 s and 15 accumulations, utilizing a 785 nm laser and 600 lines/mm, scanning between 50 and 3500 nm. UV Raman spectra is susceptible to structural unit vibrations, enabling understanding of the alterations in fundamental structure during the synthesis of zeolite. Figure 5 presents the UV Raman spectra of zeolite synthesized after 4 h of crystallization time compared with fly ash.

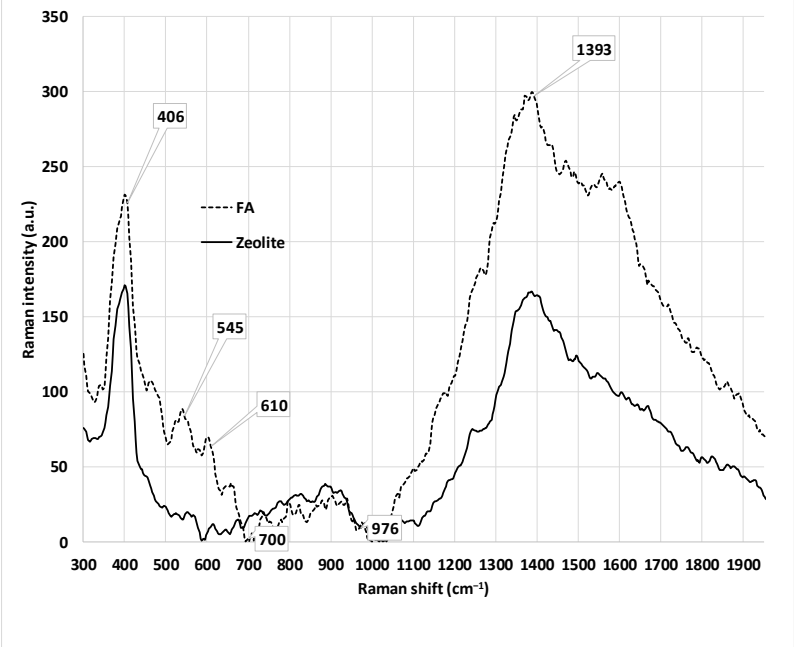

Figure 5. Raman spectra of fly ash (dashed line) and zeolite (normal line) syntheses after 4 h of crystallization.

The scanning time for the spectrum is about 40 min at room temperature and recorded in the 0–2000 cm^{-1} frequency range. Raman spectroscopy confirms the successful synthesis of zeolites from fly ash by identifying characteristic vibrational modes associated with the aluminosilicate framework. The presence of strong peaks corresponding to Si–O–Si and Al–O–Si bonds indicates effective zeolitization. Additionally, the shift in Raman bands

compared to raw fly ash reflects structural reorganization, confirming the formation of a well-defined zeolite phase.

Fly ash had a strong peak at 406 cm^{-1} and some medium and weak peaks at 545 and 610 cm^{-1}. A broad band at 406 cm^{-1} is associated with vitreous/highly polymerized silica and symmetric tetrahedral bands of silicates are larger than other high-frequency bands [35,36]. Furthermore, the bands between 700–976 cm^{-1} can be associated with the vibrations of the aluminosilicate framework and the motion of silicon (Si) and aluminum (Al) atoms within the tetrahedral structure. The Raman band in the 700–800 cm^{-1} domain is related to the symmetric stretching vibrations of the Si-O-Si/Al-O-Al bonds within the zeolite framework, while the band 900–1000 cm^{-1} confirms the asymmetric stretching vibrations of Si-O and Al-O bonds). These bands are crucial for confirming the successful formation of zeolite structures from fly ash, as they indicate the presence of characteristic aluminosilicate framework vibrations [37].

The bands present in the 1300–1500 cm^{-1} domain are often attributed to the presence of carbonate species (CO_3^{2-}) or organic residues that may remain from the synthesis process. In some cases, they can also be linked to structural defects or impurities. Additionally, the domain 1500–1600 cm^{-1} is commonly associated with adsorbed water and hydroxyl groups, particularly the bending mode of H-O-H from hydrated zeolites. It may also relate to the presence of structural hydroxyl groups (Si-OH or Al-OH).

The decrease in intensity of peaks at 406 cm^{-1} and 1393 cm^{-1}, along with the disappearance of bands at 450, 545, 610, 650, and bands from 1350–1500 cm^{-1}, indicates the removal of impurities and non-zeolitic components during acid treatment. Additionally, the increased intensity of bands between 700–976 cm^{-1} in zeolite samples suggests improved silicate framework organization, reflecting successful crystallization of the aluminosilicate gel.

3.2.6. X-Ray Diffraction Analysis

The X-ray diffraction data recorded on the synthetized powder material (Z-syn) was analyzed using the Rietveld refinement method. The zeolite-type structure was confirmed, and the key structural parameters will be discussed further. A high crystallinity degree of 95.3 ± 0.3% was found. Phase identification revealed the presence of one zeolite-type phase, sodium calcium aluminum silicate hydrate (sodalite), according to information indicated in Table 3. The result is consistent with the XRF chemical composition found (Table 2)

Table 3. Crystal structure parameters for the reference crystal zeolite considered (ICDD PDF4+, v. 2023).

Phase Name	Chemical Formula	Crystal System	Space Group	Density (g/cm^3)	ICDD-PDF Card Number
Sodium Calcium Aluminum Silicate Hydrate Zeolite name: Sodalite	$Na_4Ca_2Al_6(SiO_4)_6(H_2O)_8$	Cubic	P-43n (218)	2.35	04-014-3518

In the Figure 6 it is shown the X-ray pattern recorded for the synthesized material (Z-syn). The matching results between the measured and reference patterns showed 16 peaks, (* marked in Figure 6) which may indicate the presence of sodalite in the material obtained from flying ash wastes. One may be clearly observed the peaks at two-theta values around 14, 19, 22, 24, 28, 31, 34, 37, 42, 52, 58, 62, 64, 69, 74, 78 degrees, corresponding to Miller indices (hkl) of (110), 200, 210, 211, 220, 310, 222, 321, 411, 431, 440, 600, 532, 622, 543, 721 respectively of sodalite cubic structure. However, few peaks remain unknown after

the analysis, which indicates the presence of other phases that couldn't be identified at this point.

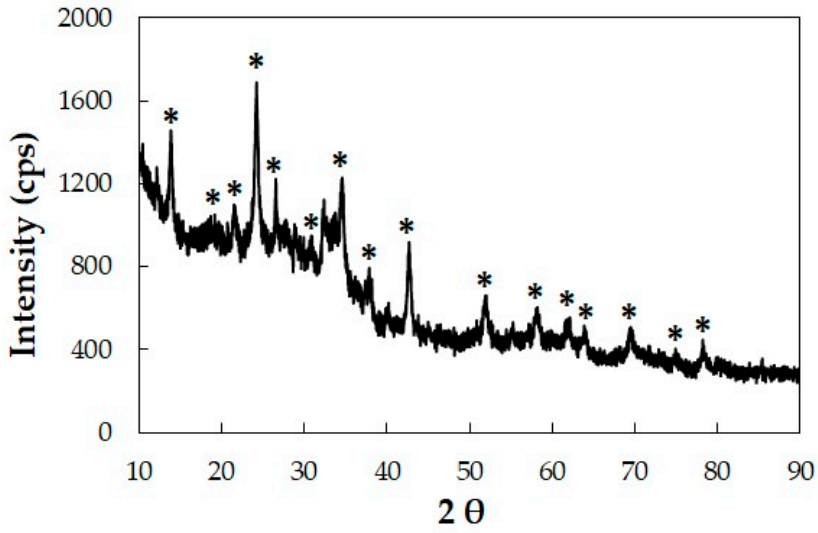

Figure 6. X-ray pattern recorded on synthesized material in Bragg Brentano geometry.

As may be noticed in Table 4, The synthesized material (Z-syn) shows structural similarity to the reference sodalite, as indicated by comparable lattice constants and angles.

Table 4. Structural parameters comparison of sample as-synthesized with reference zeolite.

Structural Parameter	Sodalite (Reference PDF 04-014-3518)	Z-syn (Synthesized Material)
V [Å^3]	717.16	723.121 (19)
a/b/c [Å]	8.951 (3)	8.97574 (13)
α/β/γ [°]	90	90
D [Å]	not available	40 (4)
S [%]	not available	0.0
d [g/cm^3]	3.386	2.304
D_{211} [Å]	3.654230	3.671 (3)

Note(s): (V—unit cell volume; a, b, c—lattice constants; D—average crystallite size, S—lattice strain, d—calculated density, D_{211}—inter-planar for the characteristic peak of 2-theta ~ 24°).

The unit cell volume, and lattice constants of Z-syn are slightly higher than that of the reference material. These data may be assigned to small expansions in the unit cell, together with structural modifications due to incorporation of different ions, defects, or impurities during synthesis.

The small crystallite size of the newly obtained material from waste flying ash, could make it suitable for applications where high surface area is desirable. The negligible strain indicates a good crystallinity and minimal defects resulted in final product after synthesis.

The lower density of the obtained Z-syn material suggests either a higher porosity, or the incorporation of lighter elements during the process.

The inter-planar distance D_{211} for the characteristic peak of 2θ around 24° has a slightly higher value compared with reference sodalite, the result being consistent with the information about the values showed in Table 4. According to the description of sample preparation in the PDF card 04-014-3518, the reference material was maintained at 220 °C for 48 h, while the synthesized material was thermally treated at 500 °C. Considering this information, another explanation for slightly higher values in the inter-planar distance D_{211} for the as-obtained material may be assigned to the thermal effect [38].

These experimental findings may influence material's functional properties, and making it a good candidate for specific practical applications where there characteristics are desirable.

3.3. Adsorption Study

3.3.1. Effect of Adsorbent Dose

Since adsorbent dose it is an important factor that can influence the performance of adsorption process, various amounts of zeolite (from 0.2 g/L to 4 g/L) were used in order to determine removal efficiency of Ni^{2+} and Cd^{2+} from aqueous solutions. Initial concentrations of solutions were 30 mg/L (for Ni^{2+}) and 35 mg/L (for Cd^{2+}). Contact time was set at 30 min for all experiments. The adsorption of the metals was studied using standard solutions (Certified Reference Materials) of Ni^{2+} and Cd^{2+}.

Experimental results presented in Figure 7 shows that for both Ni^{2+} and Cd^{2+} removal efficiency increases with the increase of specific surface area. On the other hand, a zeolite dose of 2 g/L assures the removal of Ni^{2+} and Cd^{2+} from aqueous solutions with efficiency more than 90%. Increasing the adsorbent dose to 4 g/L led only to a small increase of removal efficiencies. Therefore a adsorbent dose of 2 g/L was considered optimum and used in further experiments

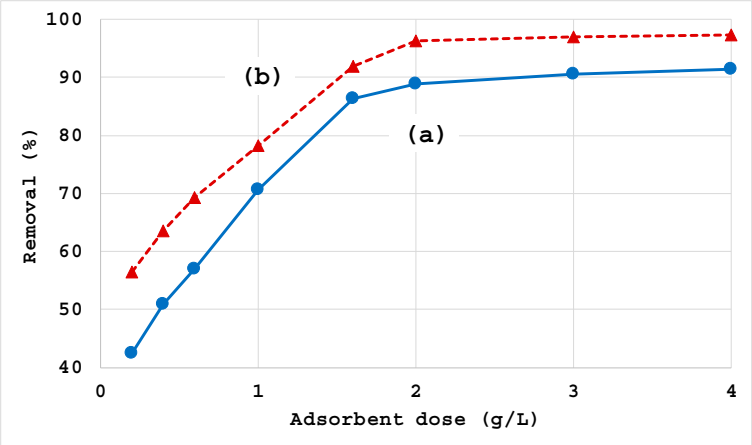

Figure 7. Effect of adsorbent dosage on Ni^{2+} (a) and Cd^{2+} (b) removal, initial concentration Ni^{2+} = 30 mg/L, initial concentration Cd^{2+} = 35 mg/L, contact time = 30 min, pH = 7.

3.3.2. Effect of pH

pH represents another key parameter that influences removal efficiency. The effect of pH on removal efficiency is presented within Figure 8.

In the case of Ni^{2+} removal, the efficiency increases with the increase of the pH. There is a high increase of removal efficiency when pH increases from 2 to 8 that can be explained by the fact that at low pH there is a competition between Ni^{2+} and H^{+} that affects the adsorption process.

On the other hand when pH increases and solution become alkaline the precipitation of $Ni(OH)_2$ occurs [34]. In the case of Cd^{2+} removal, with the increase of pH, similar with the Ni^{2+} case, resulted in an increase of removal efficiency. However at pH values higher than 7 a decrease of adsorption was observed that can be attributed to the cadmium low solubility at high pH.

Therefore in order to study the adsorption of both Ni^{2+} and Cd^{2+} ions and eliminate the effects of competitive adsorption, nickel hydroxide precipitation and low solubility of cadmium at high pH, a pH = 7 was selected for further experiments.

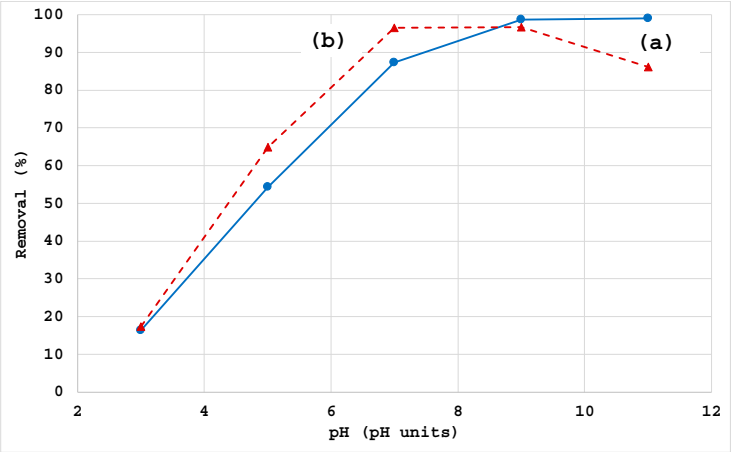

Figure 8. Effect of pH on Ni^{2+} (a) and Cd^{2+} (b) removal, initial concentration Ni^{2+} = 30 mg/L, initial concentration Cd^{2+} = 35 mg/L, contact time = 30 min; adsorbent dose = 2 g/L.

3.3.3. Sorption Isotherms

The synthesized zeolite was used to study the removal efficiency of metal ions from aqueous solutions. The metal ion solutions of known concentrations were placed in 250 mL beakers with stirring at 250 rpm and room temperature. The pH was adjusted to 7.

In order to highlight the adsorption isotherms, a constant amount of zeolite corresponding to an adsorbent dose of 2 g/L was used in addition to those mentioned above. The concentration of the starting solutions ranged from 4 to 110 mg/L for aqueous solutions containing Ni^{2+} and from 4.5 to 120 mg/L for Cd^{2+}. The slurry was kept on a rotary shaker at a constant stirring speed of 250 rpm for a certain period of time and then filtered. The resulting solutions were analyzed for heavy metals by Atomic Adsorption Spectrometry.

The interactions between metallic ions and the adsorbent were studied using the Langmuir equation with Lineweaver-Burk and Hanes-Woolf form and the influence of contact time on the adsorption capacity after 30 min and 60 min (Table 5, Figures 9 and 10). It was found that the adsorption isotherm that best describes the adsorption in the case of Ni^{2+} and Cd^{2+}, is the Langmuir in Lineweaver Burk form.

Table 5. Parameters and constants of the Langmuir isotherm for Ni^{2+} and Cd^{2+}.

		Parameters Lineweaver-Burk			**Parameters Hanes-Woolf**		
Metal	**Time (min)**	**q_m (mg/g)**	**K_L (L/g)**	**R^2**	**q_m (mg/g)**	**K_L (L/g)**	**R^2**
Ni^{2+}	30	30.12	0.476	0.9825	40.00	3.024	0.9686
	60	20.62	2.389	0.9736	38.46	2.446	0.9718
Cd^{2+}	30	23.04	2.583	0.9232	73.52	3.095	0.3953
	60	27.25	10.194	0.9534	47.39	0.654	0.7671

Therefore, adsorption process follows Langmuir isotherm in Lineweaver Burk form confirming monolayer adsorption of Ni^{2+} and Cd^{2+} ions on zeolite. According to the Linewever Burk maximum adsorption of Ni^{2+} is reached after 30 min and maximum adsorption of Cd^{2+} is achieved after 60 min.

Freundlich absorption isotherm parameters for Ni^{2+} and Cd^{2+} were calculated using the linear regression method, presented in Table 6.

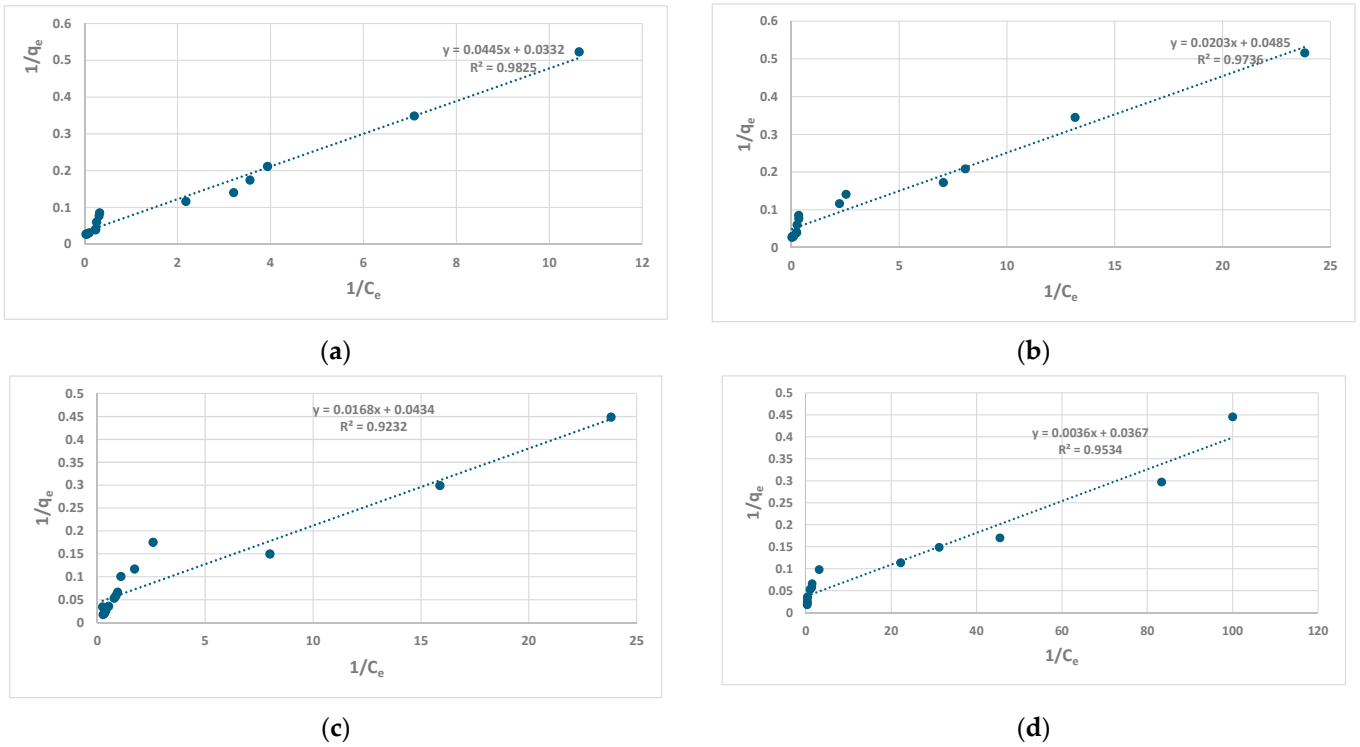

Figure 9. Lineweaver-Burk model for Ni^{2+} and Cd^{2+} adsorption capacity depending on contact time: Ni $^{2+}$ at 30 min (**a**), Ni $^{2+}$ 60 min (**b**) and for Cd^{2+} at 30 min (**c**), Cd^{2+} at 60 min (**d**), adsorbent dose = 2 g/L, pH = 7.

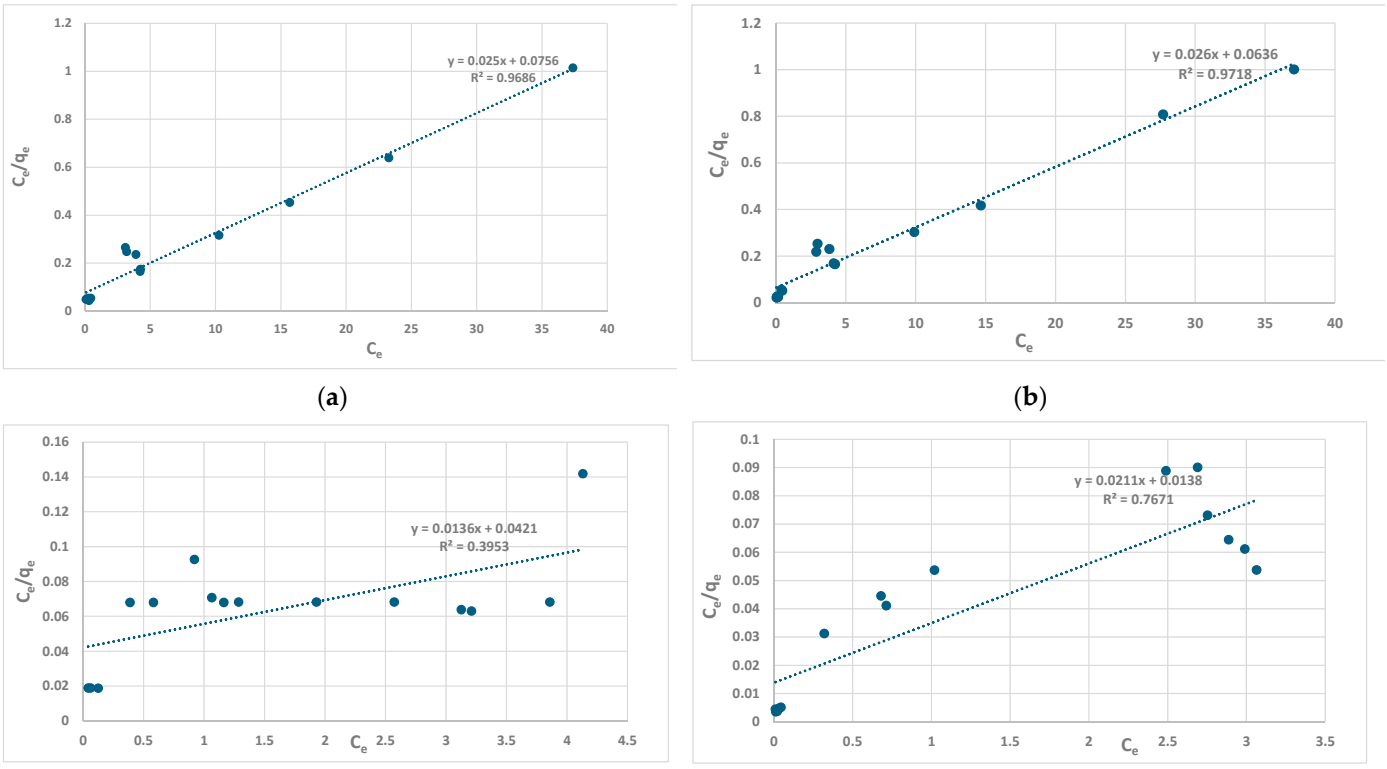

Figure 10. Hanes-Woolf model for Ni^{2+} and Cd^{2+} adsorption capacity depending on contact time: Ni^{2+} at 30 min (**a**), Ni $^{2+}$ at 60 min (**b**) and for Cd^{2+} at 30 min (**c**), Cd^{2+} at 60 min (**d**), adsorbent dose = 2 g/L, pH = 7.

Table 6. Parameters and constants of the Freundlich isotherm.

		Parameters Freundlich		
Metal	**Time (min)**	**K_F (mg/g)**	**N (L/mg)**	**R^2**
Ni^{2+}	30	0.135	2.577	0.9192
	60	0.012	3.307	0.9320
Cd^{2+}	30	0.019	1.926	0.8847
	60	0.025	2.475	0.8996

The correlation factor after 30 and 60 min contact time is represented graphical and it was observed that is better for Ni^{2+} (Figure 11a,b) rather than Cd^{2+} (Figure 11c,d).

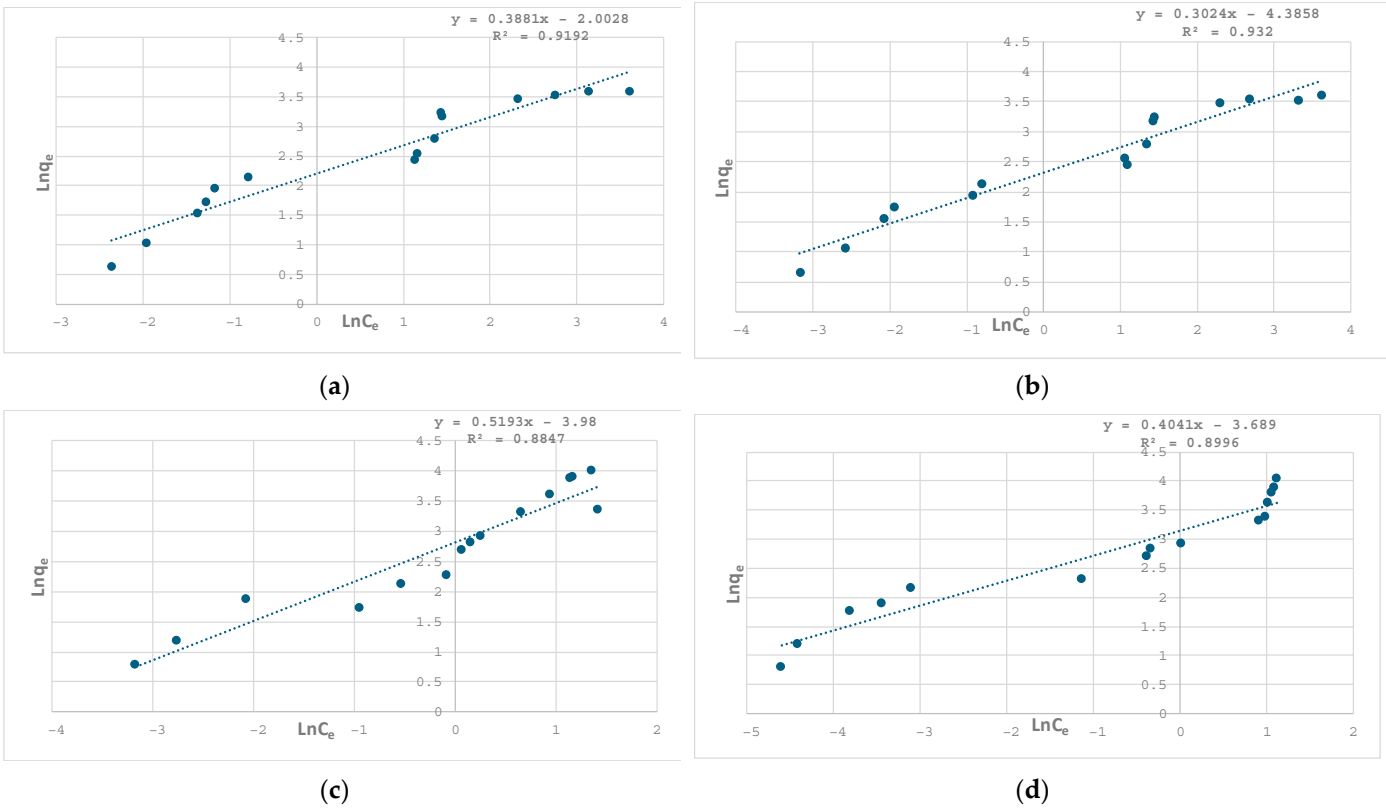

Figure 11. The correlation factor in Freundlich isotherm for Ni^{2+} at 30 min (**a**) and 60 min (**b**) and Cd^{2+} at 30 min (**c**) and 60 min (**d**), adsorbent dose = 2 g/L, pH = 7.

3.3.4. Kinetics

Kinetic modelling represents an important tool to examine the adsorption mechanism and the process speed. It was studied the influence of contact time in the removal capacity of Ni^{2+} and Cd^{2+}. Kinetic study of experimental data in the adsorption processes helps to investigate potential adsorption rate-controlling mechanisms, such as mass transfer, chemical reaction, and kinetic models. The experimental results were analyzed using pseudo-first order and pseudo-second order kinetic model (Table 7, Figure 12).

The pseudo-second order kinetic model describes well the kinetics of adsorption process. On the other hand the process is dependent on the concentration of adsorbate and the capacity of the adsorbent. Therefore, taking into consideration the solid nature of adsorbent, a pseudo-second order model is suggested. k_2 is an important parameter

and represents the adsorption rate of the heavy metals (Ni^{2+} and Cu^{2+}). The adsorption rates indicated by the k_2 values demonstrates that higher rate constants reflect increasing interaction between the adsorbate and adsorbent at the molecular level.

Table 7. Parameters for pseudo first and pseudo second order kinetic model.

		Pseudo First-Order Kinetic Parameters			Pseudo Second-Order Kinetic Parameters		
	Initial Concentration (mg/L)	**q_e (mg/g)**	**k_1 (min^{-1})**	**R^2**	**q_e (mg/g min)**	**k_2 (g/mg min)**	**R^2**
Metal							
Ni^{2+}	30	7.8686	0.0527	0.8262	13.5318	0.0910	0.9997
	110	26.1577	0.0083	0.4711	37.4532	0.0792	0.9999
Average k_1, k_2			0.0305 ± 0.0222			0.0851 ± 0.0059	
Cd^{2+}	35	6.4640	0.0426	0.8105	17.4825	0.1759	0.9999
	120	40.7287	0.0025	0.4602	57.1429	0.1801	0.9990
Average k_1, k_2			0.0226 ± 0.0200			0.1780 ± 0.0021	

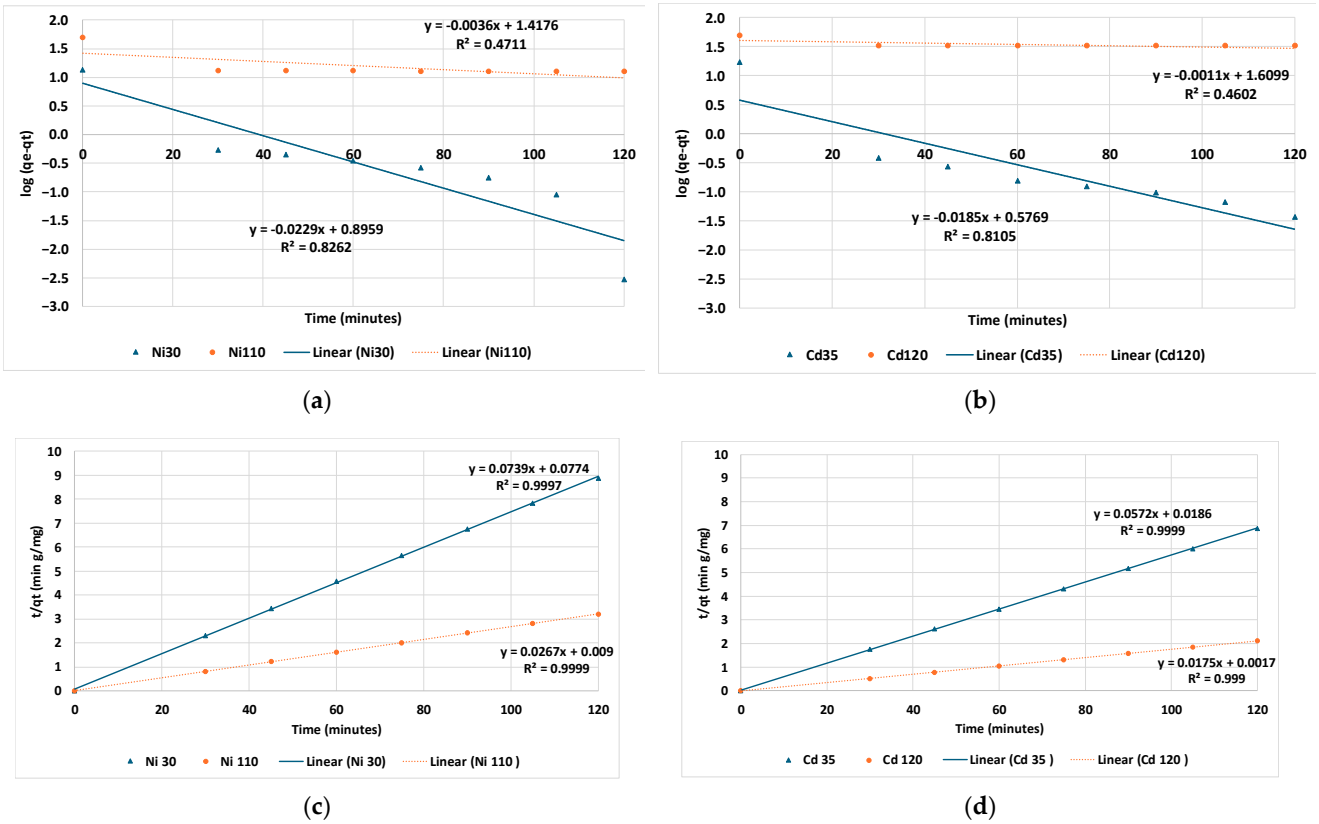

Figure 12. Correlation of experimental results with the pseudo first order kinetic model for the adsorption process of Ni^{2+} (**a**) and Cd^{2+} (**b**) and pseudo second order kinetic model for the adsorption process of Ni^{2+} (**c**) and Cd^{2+} (**d**), initial concentration Ni^{2+} = 30 and 110 mg/L, initial concentration Cd^{2+} = 35 and 120 mg/L, adsorbent dose = 2 g/L, pH = 7.

3.3.5. Interactions Involved in the Metal Adsorption Process

Phase I—Diffusion to the interface—it is a process that undergoes with high speed when the solution is mixed with the zeolite. The ions from the solution migrate toward the interface. As the interface becomes "crowded" the diffusion process slows down.

Phase II—Interaction with the Interface

Zeolites have a high specific surface area, which allows for significant adsorption of metal ions onto their surfaces. The surface of the zeolite can interact with the metal ions, providing sites for binding.

Interactions with the surface that could explain the variations of removal efficiency:

- Ni(II) and Cd(II) metal ions may form stronger complexes with specific functional groups present in the zeolite. If the zeolite has modified surfaces with functional groups or certain organic ligands, this could enhance adsorption.
- Ionic exchange is a significant mechanism for zeolites, particularly in aqueous solutions. The sodium ions (Na^+) in the zeolite structure can be substituted for metal ions like Ni^{2+} and Cd^{2+}. This exchange occurs more readily at lower pH values due to the presence of Ni^{2+}/Cd^{2+}, $Ni(OH)^+/Cd(OH)^+$ ions that could replace sodium, calcium, and magnesium ions (present in zeolite structure according to XRF analysis). When the pH value is higher the ions are replaced by $Ni(OH)_2$ and $Cd(OH)_2$ in solution which are compounds with very low solubility. Consequently, when the pH value is higher the ion exchange becomes negligible in the overall mechanism.
- At higher pH levels, metal ions might precipitate as hydroxides or other compounds, which can also contribute to the removal from solution, although this mechanism is less likely if the zeolite is effectively absorbing the ions.
- Weak van der Waals forces in addition to ionic and covalent bonds may occur, particularly at lower concentrations of metal ions, but is generally considered less impactful than chemical exchange.

The modified interaction between zeolite and Ni(II) and Cd(II) when the pH value is modified could be explained by acid-base reactions according with Pearson's HSAB Theory.

According to HSAB theory interactions between acids and bases are stronger between the species of the same hardness. Zeolites are typically considered to offer hard bases for interaction with the species adsorbed in the interface. Oxygen atoms bind to Si or Al act as a hard base due and form strong interactions with hard acids (such as Na^+ ions or alkaline earth metals) because of its strong polarizability and high electronegativity [39].

As a consequence, at low pH value, the ions Cd^{2+} (soft acid), and Ni^{2+} (borderline acid) are in competition with hydronium ions (strong acids), which are preferred by the zeolite surface. When the pH of the solution is increasing the Ni^{2+}/Cd^{2+} ions are gradually replaced by species that contain hydroxyl groups bounded with the metal atom [40]. The introduction of hydroxide ions (HO^-) can lead to the formation of hydroxo-complexes (e.g., $M(OH)^+$ or $M(OH)_2$) which can strengthen the interaction with the zeolite's surface. This transition affects the hardness of species that contain Ni/Cd, potentially making the ions more reactive in terms of adsorption. Consequently, a larger amount of transitional metals is bounded to the interface (Figure 13).

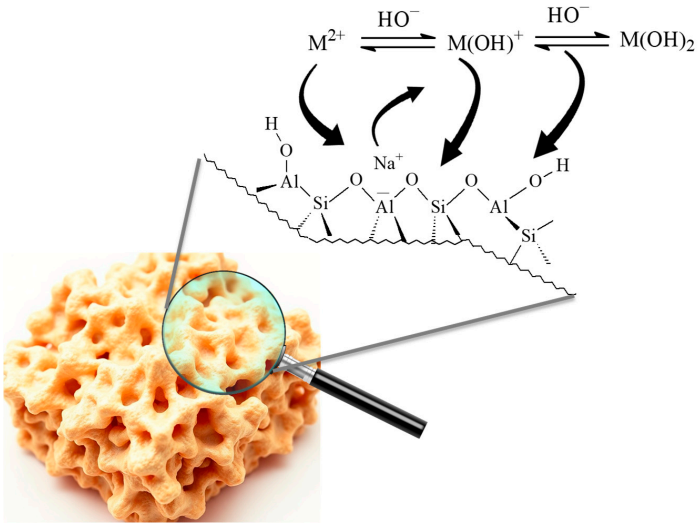

Figure 13. Interactions involved in adsorption process (M = Ni, Cd).

3.3.6. Reusability and Comparison with Other Zeolite Types

Removal efficiency of adsorbent material decreased when reused in multiple adsorption cycles. After each cycle, the zeolite was repeatedly washed with an ethanol: ultrapure water solution (1:1) and dried at 100 °C for 24 h. Ni^{2+} removal efficiency decreased from 90% (1st cycle) to less than 70% (5th cycle) since Cd^{2+} removal efficiency decreased from 96% (1st cycle) to less than 75% (5th cycle), therefore it was considered that the synthesized zeolite could be used for five cycles (Figure 14).

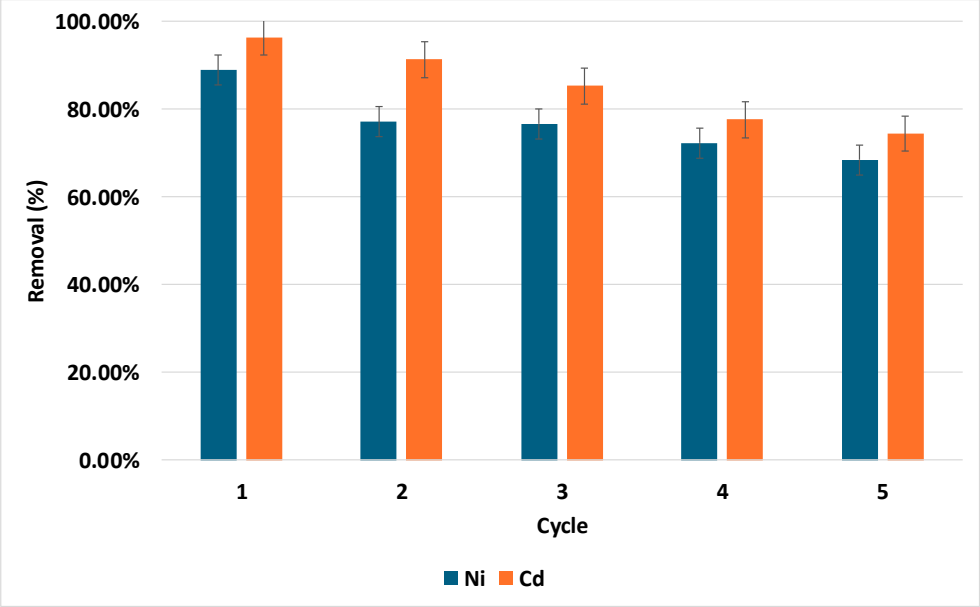

Figure 14. Zeolite reusability during five cycles, initial concentration Ni^{2+} = 30 mg/L, initial concentration Cd^{2+} = 35 mg/L, adsorbent dose = 2 g/L, pH = 7, contact time = 30 min.

Same types of adsorbent material were used in other studies for adsorption of Ni^{2+} and Cd^{2+} from aqueous systems. Table 8 presents a comparison of the results available within literature with those obtained in this study.

Table 8. Comparison of Ni^{2+} and Cd^{2+} removal using various types of zeolites.

Ion	Adsorbent	Adsorption Capacity (mg/g)	Initial Concentration (mg/L)	Adsorbent Dosage (g/L)	Reference
Ni^{2+}	Zeolite A	47	100	2	[34]
	Zeolite X	16	100	2.5	[41]
	Natural zeolite	3.4	80	2.5	[42]
	Clinoptilolite	13	80	2.5	[43]
	Zeolite synthesized from fly ash	13	30	2	This study
Cd^{2+}	Na modified zeolite—rich tuff	16.33	30	10	[44]
	Coal fly ash zeolite	52	100	1	[45]
	Natural zeolite	4	80	2.5	[42]
	Clinoptilolite	4.2	80	2.5	[43]
	Zeolite synthesized from fly ash	17	35	2	This study

The zeolite synthesized in this work presents an adsorption capacity similar with other natural or synthetic zeolites showing good adsorption performance. On the other

hand, it presents the advantage of being synthesized starting from waste fly ash, which is a cheap material.

4. Conclusions

The experimental study aimed to synthesize zeolite from fly ash and to investigate the sorption capacity in aqueous solutions for two heavy metals cations. Synthetic zeolite could be a promising material for wastewater treatment and an alternative to another adsorbents. They present good thermal stability and adsorption properties.

The synthesized zeolite was characterized by Scanning Electronic Microscopy, Fourier Transformed Infrared spectroscopy, X-ray diffraction, Raman spectroscopy, X-Ray Fluorescence and thermogravimetric analysis.

The influence of adsorbent dose and pH upon the adsorption process of Ni^{2+} and Cd^{2+} on synthesized zeolite was investigated. An adsorbent dose of 2 g/L and a neutral pH was set up for further experiments.

It was found that the adsorption isotherm that best describes the adsorption in the case of Ni^{2+} and Cd^{2+} is Langmuir in Lineweaver Burk form. According to the Lineweaver Burk form maximum adsorption for Ni^{2+} is reached after 30 min and maximum adsorption for Cd^{2+} is achieved after 60 min.

The adsorption equilibrium evaluated with the Freundlich isotherm model fitted better for Ni^{2+}, linear regression values R^2 = 0.9192 (after 30 min), 0.932 (after 60 min); as in the case of Cd^{2+}, R^2 = 0.8847 (after 30 min), 0.8996 (after 60 min).

Pseudo-second-order kinetic model correlates with the experimental data on the sorption of Cd^{2+} and Ni^{2+} ions, the correlation coefficient being close to 1. It can be assumed that this were the moments when the equilibrium in metal concentration occurred.

Reusability of synthesized zeolite was evaluated and it was found that it can be used at least for 5 cycles.

Experimental results proved that fly ash residue is a suitable and sustainable source for zeolite preparation, which can be used for removal of metal ions from aqueous media.

Author Contributions: Conceptualization, M.A.C. and L.A.C.; methodology, L.A.C.; software, V.R.B.; validation, V.R.B., C.M.N. and M.B.; formal analysis, V.R.B., C.M.N. and M.B.; investigation, M.A.C. and F.D.C.; data curation, F.D.C.; writing—original draft preparation, M.A.C., L.A.C., F.D.C., C.M.N. and M.B.; writing-review and editing, M.A.C., M.B., C.M.N. and L.A.C.; visualization, C.M.N. and M.B.; supervision, M.A.C.; project administration, M.A.C. All authors have read and agreed to the published version of the manuscript.

Funding: This work was carried out through the "Nucleu" Program within the National. Research Development and Innovation Plan 2022–2027 with the support of Romanian Ministry of Research, Innovation and Digitalization, contract no. 3N/2022, Project code PN 23 22 04 01.

Data Availability Statement: Data are contained within the article.

Conflicts of Interest: The authors declare no conflicts of interest.

References

1. Shaker, O.A.; Safwat, S.M.; Matta, M.E. Nickel removal from wastewater using electrocoagulation process with zinc electrodes under various operating conditions: Performance investigation, mechanism exploration, and cost analysis. *Environ. Sci. Pollut. Res.* **2023**, *30*, 26650–26662. [CrossRef] [PubMed]
2. Adamczyk, Z.; Białecka, B. Hydrothermal Synthesis of Zeolites from Polish Coal Fly Ash. *Polish J. Environ. Stud.* **2005**, *14*, 713–719.
3. Yoldi, M.; Fuentes-Ordoñez, E.G.; Korili, S.A.; Gil, A. Zeolite synthesis from industrial wastes. *Microporous Mesoporous Mater.* **2019**, *287*, 183. [CrossRef]
4. Boycheva, S.; Zgureva, D.; Lazarova, H.; Popova, M. Comparative studies of carbon capture onto coal fly ash zeolites Na-X and Na–Ca-X. *Chemosphere* **2021**, *271*, 129505–133225. [CrossRef] [PubMed]

5. Peng, P.; Gao, X.H.; Yan, Z.F.; Mintova, S. Diffusion and catalyst efficiency in hierarchical zeolite catalysts. *Natl. Sci. Rev.* **2020**, *7*, 1726–1742. [CrossRef]
6. Algieri, C.; Drioli, E. Zeolite membranes: Synthesis and applications. *Sep. Purif. Technol.* **2021**, *278*, 119295. [CrossRef]
7. Velarde, L.; Nabavi, M.S.; Escalera, E.; Antti, M.L.; Akhtar, F. Adsorption of heavy metals on natural zeolites: A review. *Chemosphere* **2023**, *328*, 138508. [CrossRef]
8. Tatlier, M.; Munz, G.; Henninger, S.K. Relation of water adsorption capacities of zeolites with their structural properties. *Microporous Mesoporous Mater.* **2018**, *264*, 70–75. [CrossRef]
9. Ahmed, A.A.; Yamani, Z.H. Synthesis and characterization of SnO_2-modified ZSM-5 zeolite for hydrogen gas sensing. *Materi. Chem. Phys.* **2021**, *259*, 124181. [CrossRef]
10. Abdelwahab, O.; Thabet, W.M. Natural zeolites and zeolite composites for heavy metal removal from contaminated water and their applications in aquaculture Systems: A review. *Egypt. J. Aquat. Res.* **2023**, *49*, 431–443. [CrossRef]
11. Tran, H.N.; Viet, P.V.; Chao, H.P. Surfactant modified zeolite as amphiphilic and dual-electronic adsorbent for removal of cationic and oxyanionic metal ions and organic compounds. *Ecotoxicol. Environ. Saf.* **2018**, *147*, 55–63. [CrossRef]
12. Wołowiec, M.; Muir, B.; Zieba, K.; Bajda, T.; Kowalik, M.; Franus, W. Experimental study on the removal of VOCs and PAHs by zeolites and surfactant-modified zeolites. *Energy Fuels* **2017**, *31*, 8803–8812. [CrossRef]
13. Mokrzycki, J.; Fedyna, M.; Marzec, M.; Szerement, J.; Panek, R.; Klimek, A.; Bajda, T.; Mierzwa-Hersztek, M. Copper Ion-exchanged zeolite X from fly ash as an efficient adsorbent of phosphate ions from aqueous solutions. *J. Environ. Chem. Eng.* **2022**, *10*, 108567. [CrossRef]
14. Andrunik, M.; Bajda, T. Removal of pesticides from waters by adsorption: Comparison between synthetic zeolites and mesoporous silica materials. A Review. *Materials* **2021**, *14*, 3532. [CrossRef] [PubMed]
15. Andrunik, M.; Skalny, M.; Bajda, T. Functionalized adsorbents resulting from the transformation of fly ash: Characterization, modification, and adsorption of Pesticides. *Sep. Purif. Technol.* **2023**, *309*, 123106. [CrossRef]
16. Mokrzycki, J.; Franus, W.; Panek, R.; Sobczyk, M.; Rusiniak, P.; Szerement, J.; Jarosz, R.; Marcinska-Mazur, L.; Bajda, T.; Mierzwa-Hersztek, M. Zeolite composite materials from fly ash: An assessment of physicochemical and adsorption properties. *Materials* **2023**, *16*, 2142. [CrossRef]
17. Wolny-Koladka, K.; Jarosz, R.; Marcinska-Mazur, L.; Lošák, T.; Mierzwa-Hersztek, M. Effect of mineral and organic additions on soil microbial composition. *Int. Agrophysics* **2022**, *36*, 131–138. [CrossRef]
18. Rani, L.; Kaushal, J.; Srivastav, A.L.; Mahajan, P. A critical review on recent developments in MOF adsorbents for the elimination of toxic metals from aqueous solutions. *Environ. Sci. Pollut. Res.* **2020**, *27*, 44771–44796. [CrossRef]
19. Abidli, A.; Rejeb, Z.B.; Zaoui, A.; Naguib, H.E.; Park, C.B. Comprehensive insights into the application of graphene-based aerogels for metals removal from aqueous media: Surface chemistry, mechanisms, and key features. *Adv. Colloid Interface Sci.* **2025**, *335*, 103338. [CrossRef]
20. Grabias-Blicharz, E.; Panek, R.; Franus, M.; Franus, W. Mechanochemically assisted coal fly ash conversion into zeolite. *Materials* **2022**, *15*, 7174. [CrossRef]
21. Grela, A.; Kuc, J.; Klimek, A.; Matusik, J.; Pamuła, J.; Franus, W.; Urbanski, K.; Bajda, T. Erythromycin scavenging from aqueous solutions by zeolitic materials derived from fly ash. *Molecules* **2023**, *28*, 798. [CrossRef] [PubMed]
22. Verdoliva, V.; Saviano, M.; De Luca, S. Zeolites as acid/basic solid catalysts: Recent synthetic developments. *Catalysts* **2019**, *9*, 248. [CrossRef]
23. Längauer, D.; Cablík, V.; Hredzák, S.; Zubrik, A.; Matik, M.; Danková, Z. Preparation of synthetic zeolites from coal fly ash by hydrothermal synthesis. *Materials* **2021**, *14*, 1267. [CrossRef] [PubMed]
24. Nasser, G.A.; Muraza, O.; Nishitoba, T.; Malaibari, Z.; Yamani, Z.H.; Al-Shammari, T.K.; Yokoi, T. Microwave-assisted hydrothermal synthesis of CHA zeolite for methanol-to-olefins reaction. *Ind. Eng. Chem. Res.* **2018**, *58*, 60–68. [CrossRef]
25. Park, J.W.; Kim, S.S.; Lee, W.K.; Lee, C.H. Optimization of crystallization parameters for synthesis of zeolitic materials from coal fly ash using fusion/hydrothermal method. *Mol. Cryst. Liq. Cryst.* **2020**, *704*, 136–144. [CrossRef]
26. Aldahri, T.H. Microwave and Ultrasonic Assisted Synthesis of Zeolites from Coal Fly Ash in Batch and Circulating Batch Operation. Ph.D. Thesis, The University of Western Ontario, London, ON, Canada, 2019. Available online: https://ir.lib.uwo.ca/etd/6168 (accessed on 7 January 2025).
27. Burakov, A.E.; Galunin, E.V.; Burakova, I.V.; Kucherova, A.E.; Agarwal, S.; Tkachev, A.G.; Gupta, V.K. Adsorption of heavy metals on conventional and nanostructured materials for wastewater treatment purposes: A review. *Ecotoxicol. Environ. Saf.* **2018**, *148*, 702–712. [CrossRef]
28. Raji, Z.; Karim, A.; Karam, A.; Khalloufi, S. A review on the heavy metal adsorption capacity of dietary fibers derived from agro-based wastes: Opportunities and challenges for practical applications in the food industry. *Trends Food Sci. Technol.* **2023**, *137*, 74–91. [CrossRef]
29. Xiaoyu, Z.; Chunquan, L.; Shuilin, Z.; Yonghao, D.; Zhiming, S. A review of the synthesis and application of zeolites from coal-based solid wastes. *Int. J. Miner. Metall. Mater.* **2022**, *29*, 1–21. [CrossRef]

30. Agata, M.M. Recent findings on fly ash-derived zeolites Synthesis and utilization according to the circular economy concept. *Energies* **2023**, *16*, 6593. [CrossRef]
31. Parra-Huertas, R.A.; Calderón-Carvajal, C.O.; Gómez-Cuaspud, J.A.; Vera-López, E. Synthesis and characterization of Faujasite-Na from fly ash by the fusion-hydrothermal method. *Boletín Soc. Española Cerámica Vidr.* **2023**, *62*, 527–542. [CrossRef]
32. Constantinov, F.D.; Constantin, M.A.; Puiu, D.; Ionescu, I.A.; Cernica, G. Surveying, Geology and Mining, Ecology and Management. In Proceedings of the 23rd International Multidisciplinary Scientific GeoConference (SGEM 2023), Vienna, Austria, 28 November–1 December 2023. [CrossRef]
33. Osmari, T.A.; Gallon, R.; Schwaab, M.; Barbosa-Coutinho, E.; Severo, J.B., Jr.; Pinto, J.C. Statistical analysis of linear and non-linear regression for the estimation of adsorption isotherm parameters. *Adsorpt. Sci. Technol.* **2013**, *31*, 433–458. [CrossRef]
34. He, X.; Yao, B.; Xia, Y.; Huang, H.; Gan, Y.; Zhang, W. Coal fly ash derived zeolite for highly efficient removal of Ni^{2+} in waste water. *Powder Technol.* **2020**, *367*, 40–46. [CrossRef]
35. Witte, A.; Garg, N. Particle shape, crystallinity, and degree of polymerization of fly ash via combined SEM-EDS and Raman spectroscopy. *Cem. Concr. Res.* **2024**, *184*, 107612. [CrossRef]
36. Visa, M. Synthesis and characterization of new zeolite materials obtained from fly ash for heavy metals removal in advanced wastewater treatment. *Powder Technol.* **2016**, *294*, 338–347. [CrossRef]
37. Tsai, Y.L.; Huang, E.; Li, Y.H.; Hung, H.T.; Jiang, J.H.; Liu, T.C.; Fang, J.N.; Chen, H.F. Raman spectroscopic characteristics of zeolite group minerals. *Minerals* **2021**, *11*, 167. [CrossRef]
38. Cullity, B.D.; Stock, S.R. *Elements of X-Ray Diffraction*, 3rd ed.; Pearson New International Edition: Harlow, UK, 2014.
39. Pearson, R.G. Hard and soft acids and bases, HSAB, part 1: Fundamental principles. *J. Chem. Educ.* **1968**, *45*, 581. [CrossRef]
40. Liang, Y.M.; Jun, M.; Liu, W. Enhanced removal of lead (II) and cadmium (II) from water in alum coagulation by ferrate (VI) pretreatment. *Water Environ. Res.* **2007**, *79*, 2420–2426. [CrossRef]
41. Zhang, Y.; Dong, J.; Guo, F.; Shao, Z.; Wu, J. Zeolite synthesized from coal fly ash produced by a gasification process for Ni^{2+} removal from water. *Minerals* **2018**, *8*, 116. [CrossRef]
42. Merrikhpour, H.; Jalali, M. Comparative and competitive adsorption of cadmium, copper, nickel, and lead by Iranian natural zeolite. *Clean Technol. Environ. Policy* **2013**, *15*, 303–316. [CrossRef]
43. Sprynskyy, M.; Buszewski, B.; Terzyk, A.P.; Namiesnik, J. Study of the selection mechanism of heavy metal (Pb^{2+}, Cu^{2+}, Ni^{2+}, and Cd^{2+}) adsorption on clinoptilolite. *J. Colloid Interface Sci.* **2006**, *304*, 21–28. [CrossRef]
44. Perfecto, B.P.; Guadelupe-Macedo, M.M.; Olguin, M.T. Cadmium sorption by sodium and thiourea-modified zeolite rich tuffs. *J. Environ. Sci.* **2017**, *52*, 39–48. [CrossRef]
45. He, K.; Chen, Y.; Tang, Z.; Hu, Y. Removal of heavy metal ions from aqueous solution by zeolite synthesized from fly ash. *Environ. Sci. Pollut. Res.* **2016**, *23*, 2778–2788. [CrossRef] [PubMed]